

**SEDIMENTARY TRANSPORT INFLUENCES ON
DIAGENETIC PROCESSES AT THE AMAZON
CONTINENTAL SHELF, BRAZIL**

ABSTRACT

This research aimed to correlate the sedimentary transport with the diagenetic processes in the coastal zone and Amazon Continental Shelf (ACS). Physical and physical-chemical parameters, trace element contents (Cr, Pb, Ni, Zn and Hg), and O₂, CO₂ and iron flux were determined in sediment and pore water. Sedimentary incubation (96 hours) and algorithms were applied to determine the variation of the activity coefficient (ΔI) and ionic strength (F_i) of the predominant chemical species, and to estimate the net production and mineralization of the organic matter (ΔCO_{2T}) in the system. There are not many studies applying incubation tests to identify the diagenetic processes, especially in fluvial-marines sediments. The results showed a strong zonation associated to the transport and deposition processes, influenced mainly by the grain-size and texture of sediment and fluvial streams. The distribution of trace elements followed the trend of the sedimentary pattern, with higher levels of metals in the deposits of clay minerals and organic matter. A factor of weight (F_w), calculated to establish the degree of importance of each parameter under the distribution and mobility of trace elements, suggests that the mobility of Cr, Ni and Zn is controlled by depth, clay and organic compounds contents, and concentration of dissolved oxygen. The vertical flow of O₂ and CO₂ and the Fe²⁺/Fe³⁺ ratio in the pore water suggest a predominance of organic matter oxidation in the sedimentary layer between 0.0 and 0.2 m, with partially anaerobic mineralization of the sediments below 0.4 m. Increases in trace element concentrations were observed in iron reduction zones, indicating processes of desorption of oxides and hydroxides of Fe and mineralization of organic matter. The extrapolation of the results of the incubation test to the studied system allowed to establish three hypotheses related to the diagenetic processes: 1) the flow of marine currents may be allowing the aerobic oxidation in the sandy sediments, with the nitrification route more accentuated than the ammonification route; 2) in the region of the coastal zone and inner continental shelf the routes of oxidation and reduction may be alternating according to the physical-chemical factors and seasonality; 3) in the coastal zone and inner shelf the net mineralization rate exceeded the net production rate of the organic matter ($\Delta CO_{2T} > 0$).

Keywords: pore water; trace elements; organic matter; mineralization; net productivity; Amazon Continental Shelf.

1. INTRODUCTION

The sedimentary transport regime analysis is much applied in association with geochemistry in quantitative studies, revealing areas of cumulative tendency or sedimentary dispersion. Studies have demonstrated that the sedimentation rate associated with microbiological activity, organic carbon content and seasonal events affect the concentration of dissolved

20 chemical species directly in the sediments [1,2], especially in water [3,4], which justifies the
21 influence of sedimentary transport on the diagenetic regime, with particular emphasis on
22 quantifying the seasonal rates and spatial patterns of carbon remineralization.

23 Pore water can be interpreted as a physical-chemical and biological transition phase
24 between what happens in the water and sediment compartments. This suggests a
25 complexity of factors and processes acting jointly in the genesis and flow of chemical
26 species, either by diffusion, advection, precipitation and/or dissolution of minerals, metallic
27 adsorption/desorption, bioturbation, production or mineralization of organic matter [4-6]. The
28 composition (clay and organic matter), physical (porosity) and physical-chemical properties
29 (pH and alkalinity) of the sediments influence in the diffusion and transport of the chemical
30 species in the pore water [5-7], either by vertical or horizontal movements.

31 In the region between the Amazon and Pará mouths, and the Amazon Continental Shelf
32 (ACS; Fig. 1), the sedimentary dynamics is the largest in the world, both in volume and
33 dispersion area. The distributions of minerals in ACS sediments [8], as well as organic and
34 inorganic components, including trace elements [9], are of unequal proportions to any
35 other fluvial-marine system on the planet. Fluvial-marine currents play an important role in
36 this sedimentary dynamics, acting individually or together, and seasonally in the Amazonian
37 system. The balance between the erosion, transport and sedimentation processes interferes
38 with the volume of sediments and, consequently, with the concentration of chemical species
39 in the fluvial-marine system. The Amazon River presents the highest suspended solids load
40 transported in the world, about 1.2×10^9 metric tons/year of sedimentary debris to its lower
41 reaches [10], and that once reaching the continental shelf will submit to a coastal dynamic,
42 mainly by the influence of the North Brazilian Current (NBC) along the American continent.
43 **That** sedimentary load representing ~3% of the global riverine particle flux, accumulates off
44 the river mouth in Brazilian coastal waters as deltaic mud deposits having a northwest
45 trending strike [11].

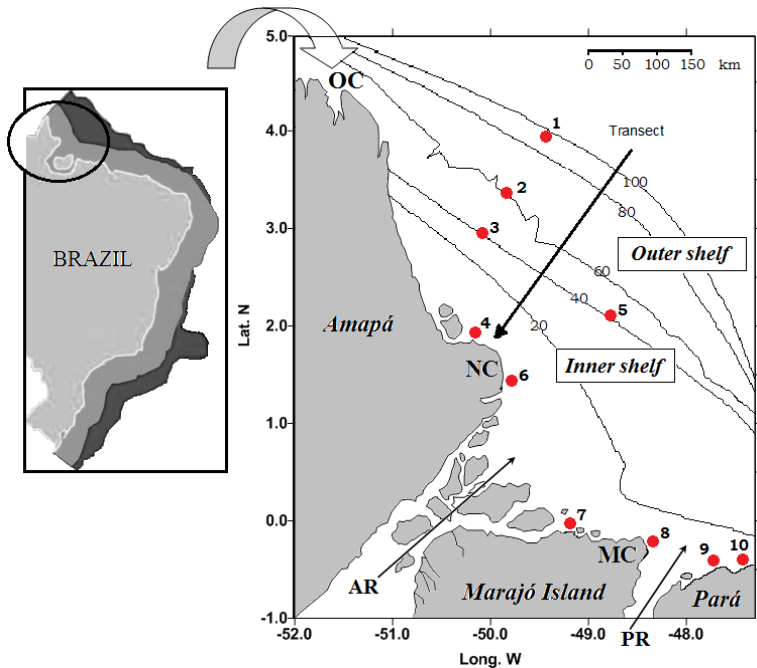
46 Diagenetic reactions and sediment-water exchange processes occurring in deposits of the
47 ACS determining the eventual influence of the Amazon on a range of marine elemental
48 cycles and characteristics of the resulting sediment record [12]. The diagenetic processes
49 involve the genesis of chemical species with consequent alteration in these compositions in
50 the environment. Among the processes involved in diagenesis, the net production and
51 mineralization of organic matter have been highlighted in geochemical studies, as they
52 interfere in the flow and balance of gases (CO_2 , O_2 , CH_4 , H_2S and SO_4^{2-}) in the water and
53 sediment compartments, in the metallic mobilization, and in the aerobic and anaerobic
54 benthic microbial productivity.

55 This research aimed to correlate the sedimentary transport with the diagenetic processes in
56 the area between the coastal zone and outer shelf of the ACS. For this, 1) the distribution
57 and flow of trace elements (Cr, Pb, Ni, Zn and Hg); 2) the profile of the vertical flow of O_2
58 and CO_2 in the pore waters, relating them to the iron redox potential (Fe^{2+} and Fe^{3+}); and 3)
59 net production and mineralization of organic matter, identifying the dominant pathway in the
60 pore water system were determined and/or estimated.

61 **2. STUDY AREA**

62 The study has been conducted in the Amazon River, nearby coastal zone (CZ) and Amazon
63 Continental Shelf – ACS ($47^\circ 52' \text{W}$ - $4^\circ 19' \text{N}$ and $51^\circ 04' \text{W}$ - $2^\circ 16' \text{S}$) between Orange Cape
64 (State of Amapá) and Pará River mouth (State of Pará, Fig. 1). It is a dynamic region,
65 influenced by the meeting of continental waters with the Atlantic Ocean on influence at the
66 Equatorial North Current (ENC) and NBC. There is also interference from atmospheric

67 forces as the Intertropical Convergence Zone (ICZ), generating trade winds and rainfall,
 68 which determining the climatic seasons and the hydrological pattern of Amazonian rivers [8].
 69 This complex system of water circulation influences sediment transport and deposition,
 70 acting in a selective way to separate the sedimentary fractions and the content of organic
 71 material by zonation in the coastal zone and ACS. The climate of the region is "Am" hot and
 72 constantly humid (monsoon climate) for Marajó Bay, and "Af" equatorial for Amazon and
 73 Pará mouths, with mean temperature of 28 °C and rainfall exceeding 2000 mm/year,
 74 especially between the months of December and February. The Amazon coastal zone
 75 includes diverse ecosystems as mangroves, dunes, coastal forests, freshwater coastal,
 76 estuaries and river deltas with great aquatic and terrestrial biodiversity associated.
 77 Descriptions of the study area and sedimentary patterns can be found in [8,9,11,13].



78

79 **Fig 1. Map of the ACS and coastal zone between Orange Cape (OC) and Pará River**
 80 **mouth. Details of the shelf – coastal zone vector 1 – 4 (transect).** Legend: NC= North
 81 Cape; MC= Maguari Cape; AR=Amazon River; PR= Pará River; isobaths in meters.

82 3. MATERIALS AND METHODS

83 Physical-chemical, water column hydrography and sedimentary load measurements were
 84 made following the regime of seasonality in the region. The bathymetric lines (isobaths)
 85 showed in the figure 1 were obtained from probe eco-bathymetry and for consultations to
 86 nautical charts. A tendency line (exponential fitting curve) with the respective differential
 87 equations was determined for the bathymetric profile, with orientation axis from the coastal
 88 zone in direction to outer shelf. The sediment samplings, however, were performed during
 89 the months of lowest flow (May and June) in the Amazon and Pará rivers and at the ACS.
 90 Samples of bottom sediments (0.0 - 0.5 m) were obtained between the 5 and 100 m
 91 isobaths using Van-Veen sampler ($A=682 \text{ cm}^2$) to the bottom sediments, and box-core
 92 sampler ($A=177 \text{ cm}^2$) to the vertical samples. The sediment samples were stored in plastic
 93 bags and kept in freezer at $-5 \text{ }^\circ\text{C}$ until the analysis. Vertical samples were used to determine
 94 the pH, salinity (u.s.) and dissolved oxygen ($\text{DO } \mu\text{mol/L}$) in the pore water.

95 At chemistry laboratories at Pará Federal University (UFPA) and National Institute of
96 Research in Amazonian (INPA), the sediment samples used for geochemical analysis were
97 fractionated, oven dried (45 ± 0.5 °C) and homogenized, sieved and pulverized until very fine
98 sand fraction ($125 - 63$ vfs μm). The pH of the samples was neutralized with 2M NH_4OH
99 solution and 30 mL of Mil-Q water followed by titration of the chloride, to ensure no
100 interference of the Cl^- analyzes. For the incubation test, fresh samples were homogenized
101 and stored in polyethylene bottles with a sealed acrylic lid. DO and CO_2 were determined
102 with probes and analytical methods (titration) from the extraction of the pore water, and
103 profiles of oxygen (DO $\mu\text{mol/L}$) and total CO_2 (ΣCO_2 mmol/L) were established in the vertical
104 layer of the sediments sampled for the vector 1 – 4 (Fig. 1).

105 Grain-size analysis was determined by the gravimetric method [14]. Organic matter (OM)
106 was determined by hot acidic extraction with excess hydrogen peroxide (30%) at 100 °C
107 [15]. The organic carbon content (OC) was determined by the Walkley-Black method [16],
108 where the organic carbon of the sample is oxidized to CO_2 with potassium dichromate
109 [$\text{K}_2\text{Cr}_2\text{O}_7$] and concentrated sulfuric acid [H_2SO_4]. The chromium of the extractive solution is
110 reduced to Cr^{3+} , and the excess of potassium dichromate is titrated by the ammonium iron
111 (II) sulfate [$(\text{NH}_4)_2\text{Fe}(\text{SO}_4)_2 \cdot 6\text{H}_2\text{O}$]. The calculation is done by applying equation 1 [14]. Free
112 CO_2 ($\text{CO}_{2\text{L}}$ mmol/L) and total CO_2 ($\text{CO}_{2\text{T}}$ mmol/L) were determinates with probe and also
113 obtained analytically by titrimetric method 4500- CO_2 A and D [17]. The titration was
114 performed potentiometrically with NaOH to bring the sample to pH 8.3 and HCl to pH 4.3.
115 From the results, the carbonate and bicarbonate alkalinities also were calculated. Inorganic
116 carbon (IC) was calculated from the amount of total CO_2 per molar transformation [15].

117
$$OC = 0.06V(40 - V_a \times f) \quad (eq.1)$$

118 Where: OC (g/kg); V = volume of potassium dichromate and V_a = volume of ammonium iron(II) sulfate
119 consumed in the reaction; f = 40/ volume of ammonium iron(II) sulfate used in the blank titration; 0.06 =
120 correction factor.

121 Trace metals Cr, Pb, Ni and Zn (mg/kg) were extracted using mixture [HNO_3 +
122 HCl]: HClO_4 :HF (Merck 2:1:1) in an open system and determined in a flame atomic
123 absorption spectrometry Shimadzu AA 6800 (Standard Method 3111B modified) [17]. Total
124 Hg (ng/g) was extracted adding dry sediment and V_2O_5 (1:1) and after a solution of
125 HCl: HNO_3 : H_2SO_4 (Merck 3:1:6) in a test tube closed, and determined in cold-vapor atomic
126 absorption (Standard Method 3112B and 3500-HgB adapted) [17]. For analytical quality
127 control, the recovery levels of acid digestion and determination of metals were tested using
128 certified reference material (SRM 2710 near-shore seawater, National Research Council of
129 Canada) analyzed in triplicate. The determinations of the total and reduced iron (Fe^{2+})
130 fractions were obtained from the methods described by [14,15]. By mass difference the Fe^{3+}
131 fraction was calculated and $\text{Fe}^{2+}/\text{Fe}^{3+}$ ratio was established. The oxidation potential of the
132 solid-reactive phase of the iron in the sediments was estimated by leaching wet sediment in
133 6N HCl for 15 minutes at 22°C (10:1 mg sediment/ ml HCl) and analyzing the leachate for
134 total Fe and Fe^{2+} .

135 The river hydrographic states were used to identify seasonal sampling times, and the
136 respective seasonality. Sampling of the coastal zone and ACS were designed to include a
137 range of major environmental conditions corresponding to changes in likely sedimentation
138 patterns, Amazon River and Para River flows, trade wind stress, and influence of the
139 Equatorial North Current and North Brazil Current (NBC). The study of the diagenetic
140 processes was concentrated at the sampling sites inserted in the vector 1 – 4 (Figure 1),
141 starting at the deepest local (site 1), near the isobath 100 meters, and ending at the coastal
142 zone (site 4), already under influence of the river currents. The sedimentary transport regime

143 was identified by the analysis of the tendency of space-time clustering of the sedimentary
 144 fractions. To estimate diffusive sedimentary flux, the incubation method described by [18]
 145 was used. In order to estimate potential diffuse exchange rates and the rates of net
 146 production and mineralization of organic matter, samples stored in the sealed vials were
 147 shaken vigorously for 5 minutes and then allowed to stand at 20 ± 0.5 °C and light/dark
 148 phases controlled for 4 days (96h). Pore water samples were removed of the sealed vials at
 149 incubation times $t_0=0h$ and $t_7=96h$ with a syringe to estimate CO_{2L} and CO_{2T} contents,
 150 according to the analytical protocols described by [15,17]. Preliminary tests showed that
 151 after four days is more difficult to estimate the diffuse sedimentary flux for the adopted
 152 method as well as for the conditions at the ACS, especially in the coastal zone with high OM
 153 levels. This occurs because the DO levels after four days are very low almost imperceptible.
 154 Thus, a maximum time of measure of four days or 96 hours was established ($t_0=0h$ and
 155 $t_7=96h$ in equation 4). Diffusive fluxes of the sediments were calculated from flux (vertical
 156 sampling from box core) by dividing the slope of a least squares line fit of the total mass
 157 change of a solute at time 't' in overlying water versus elapsed incubation time by the area of
 158 the flux core. For this study the close system method was adopted for incubation tests (to
 159 see item 4.4 Sedimentary incubation). Pore water samples were collected and analyzed for
 160 DO and CO_{2T} according to methods already decripted. The DO and CO_2 curves of
 161 consumption/ production in function of the time (Δt) are determined, suggesting the speed of
 162 the reaction of the diffuse flux (slow - moderate - fast). Exchange liquid flux by diffusion at
 163 the water-sediment interface can be estimated from tables according to temperature and
 164 pressure in the environment (pressure of gas diffusion). The net production is obtained from
 165 the determination of the CO_2 rates in function of the time (Δt). Using the algorithms of the
 166 software Carbmar 1 and 2, and Alcagran (Basic© and TBasic© 1994) and applying
 167 equations 2 – 7, the net production rate for $\Delta(CO_{2T})_b < 0 \Leftrightarrow \Delta(O_2)_b > 0$; net mineralization
 168 rate for $\Delta(CO_{2T})_b > 0 \Leftrightarrow \Delta(O_2)_b < 0$; and net remineralization reaction rate of the organic
 169 matter in the orientation of the vector 1 – 4 (Figure 1) were calculated.

$$I = 0.5 \times \sum_i Z_i^2 [i] \quad (eq. 2)$$

$$\text{Log}f_i = -A \times Z_i^2 \times \left[\left(\frac{I^{1/2}}{1 + I^{1/2}} \right) - 0.3I \right] \quad (eq.3)$$

$$\Delta(CO_{2T})_a = 0.5 \times (FCO_{2T}(t_0) + FCO_{2T}(t_7)) \quad (eq.4)$$

$$\Delta(CO_{2T})_b = \Delta(CO_{2T}) - \Delta(CO_{2T})_a \quad (eq.5)$$

$$C_{eq} = C + \frac{Mn}{6} + \frac{(Cr + Mo + V)}{5} + \frac{(Ni + Cu)}{15} \quad (eq.6)$$

$$\sum \Delta M(t) = [C(t) - Cc(t - \Delta t)] \times V' \quad (eq. 7)$$

171 Where: [eq.2] I= is the activity coefficient of the ionic functions; i = major ionic species with
 172 corresponding electrical charges (Z); [eq.3] f = ionic strength for A= 0.5 [19,20]; [eq.4] $(CO_{2T})_a$ =
 173 exchange liquid flux by diffusion at the water-sediment interface in the interval t, and FCO_{2T} in t_0 and t_7
 174 represent the flux of CO_2 in each moment t; [eq.5] $(CO_{2T})_b$ = net production or mineralization rate of
 175 CO_{2T} ; [eq.6] C_{eq} = represents the equivalent carbon with the element contents in %; [eq.7] C(t) = solute
 176 concentration at time t; Cc = concentration of solute corrected in the previous sample as a function of
 177 time variation (t - Δt); and V = volume of water overlying the core [18].

178 4. RESULTS AND DISCUSSION

179 4.1. Sedimentary characterization

180 Table 1 presents some relevant characteristics of the sediment and pore water determined
181 at the ACS. The granulometric analysis revealed the presence of mud sediments with high
182 percentage of fine silt and clay in the coastal zone, with variation of 80.6 – 90.6% (mean
183 $84.8\pm 3.6\%$). In the continental shelf area, not making a distinction between the influence of
184 the river and marine currents, the values had high variation, from 5.8 to 81.4% (mean
185 $53.6\pm 29.1\%$). Isolating the areas by influence of the currents, we have that the ACS inner
186 shelf (sites 3 and 5) had concentrations of fine sediments between 70.7 – 81.4% (average
187 $76.0\pm 5.3\%$); and on the outer shelf (sites 1 and 2) from 5.8 to 56.1% (mean $31.2\pm 25.5\%$).
188 The coastal zone and the inner shelf presented enrichment of the bottom sediments with fine
189 organic material originating from Amazon River sedimentary load. A similar pattern of
190 change in particle size was observed by [13,21], along the Amazon Shelf between 10 and 50
191 meter isobars above the North Cape (State of Amapá). According to the authors, the
192 transition in the sedimentary pattern extended from the interior delta of the Amazon River
193 towards the inner shelf with extensively reworked by intense tidal currents and waves. The
194 bathymetry suggests a behavior in a little negative exponential curve. In other words, the
195 increase in the depth of the coastal zone towards the ocean floor was slightly mild, with two
196 very evident areas of reduction in the inclination of the curve: first one at 40 meters and the
197 second one near 80 meters deep (Figure 2A). The trend of accumulation of fine sediments in
198 the fluvial-marine environment followed a distribution pattern, which can be explained by a
199 variation of the Gaussian curve. The sedimentation – deposition and physical-reworking
200 patterns indicated an area of maximum thickness of the thin sediment layer with
201 approximately 62 cm high and 49 km away from the coastal zone (Figure 2A). Similar
202 patterns were observed by [11,12]. Aller et al. [12] observed a layer of fine sediment
203 between 50 and 60 cm thick accumulated about 65 km from the coastline, above the North
204 Cape between 1.5° and 3.5° north latitude, which the authors identified as a result of
205 physical reworking of sediments from a circulation pattern influenced by NBC. According to
206 the authors, vertical sediment-water zonation in particle mobility and concentration are
207 therefore typically present at the region, with the relative zonal thicknesses determined
208 seasonally by the relative dominance of physical processes and sediment supply at each
209 site.

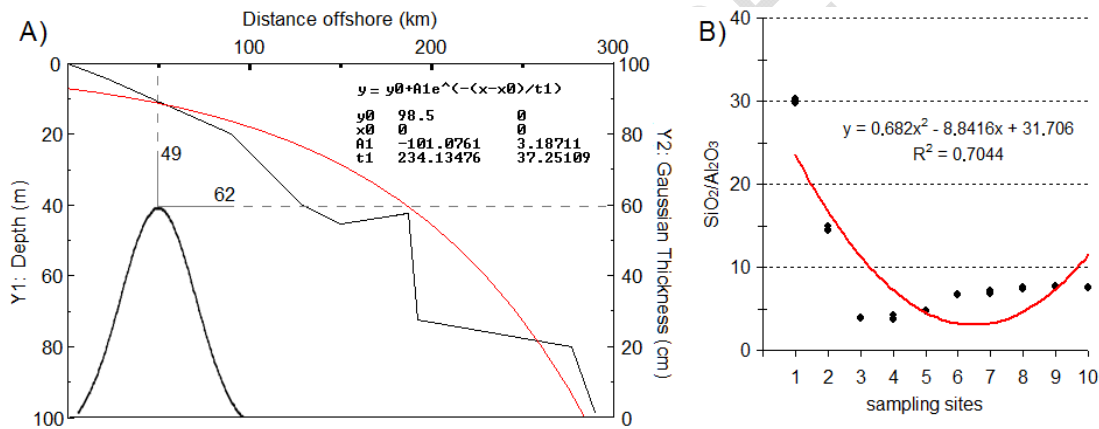
210 The organic matter (OM) and organic carbon (OC) contents in the study area varied,
211 respectively: in ACS (sites 1, 2, 3 and 5) $OM = 0.6 - 2.8\%$ (mean $1.3\pm 0.4\%$) and $OC = 0.3 -$
212 1.8% (mean $0.8\pm 0.3\%$); only on the outside of the shelf, under the influence of marine
213 currents, $OM = 0.6 - 2.8\%$ (mean $1.5\pm 0.5\%$) and $OC = 0.3 - 1.8\%$ (mean $0.8\pm 0.3\%$); in the
214 inner shelf, $OM = 1.0 - 1.6\%$ (mean $1.2\pm 0.2\%$) and $OC = 0.6 - 0.9\%$ (mean $0.7\pm 0.1\%$). As
215 expected, the coastal zone presented the highest individual OM and OC contents in the
216 sediments, varying between $OM = 2.2 - 4.9\%$ (mean $3.3\pm 0.7\%$) and $OC = 0.5 - 2.7\%$ (mean
217 $1.5\pm 0.7\%$). Most OM in water and sediment occurs as OC that has functional groups that
218 form stable complexes with trace metals, due to its capacity of cations adsorption. Thus the
219 presence of OC tends to increase the dissolved fraction of metals [22]. The decomposition of
220 OM can affect both hydrodynamic processes and geochemical redox cycles, providing
221 driving forces for metal mobilization [23]. The mobilization and distribution of trace metals in
222 water-sediment systems are dependent on physical-chemical, especially pH and redox
223 changes (DO levels), and microbiological mechanisms, mediated by the species
224 transformation [24,25], as is observed in the diagenetic processes. The physical-chemical
225 mechanisms involved include metal speciation, adsorption, precipitation, co-precipitation and
226 diffusion [22,26]. The capacity of sediments to adsorb and retain trace metals is also
227 dependent of other variables as the availability of Fe and Mn, presence of carbonate and the
228 clay minerals levels.

229 The accumulation of OM associated to fine fractions of clay increased the porosity of the
230 sediments at the coastal zone ($0.66 - 0.7 \text{ ml/cm}^3$), while in the outer shelf, owed mainly the

231 uniformity of the grain size, the sandy sediments presented the smallest porosities values
 232 (0.28 – 0.34 ml/cm³, Table 1). The porosity is defined as the amount of water that a rock or
 233 sediment can store. For this reason, porosity also can interfere in the metallic ions levels and
 234 consequent mobilization and distribution in the pore water, allowing the accumulation (stock)
 235 of metals in the sediment compartment.

236 The SiO₂/Al₂O₃ ratio followed the same trend presented for grain size, with a total variation in
 237 the study area from 3.7 (site 4) to 30.3 (site 1), and averages by zoning of 13.3±10.8 in ACS;
 238 4.3±0.5 in the inner shelf; 22.3±8.1 in outer shelf; and 6.7±1.3 in the coastal zone. These
 239 results confirm the proportion of silicates as a function of sediment transported, with a strong
 240 distinction between the low SiO₂/Al₂O₃ ratio in the sediments deposited by the fluvial
 241 currents (Amazonas and Pará rivers) and the high ratio in the sandy sediments reworked by
 242 the marines currents (Figure 2B). It is correct to say that the sediment characteristics found
 243 at each sampling site were influenced not only by the currents, but also by the depth of the
 244 bed. The shallower areas presented higher sedimentary deposition load, with accumulation
 245 of fine sediments. On the other hand, the deeper areas presented greater resuspension and
 246 swirling capacity, preventing the deposition of fine sediments.

247



248

249 **Fig. 2. A) Graphic representation of the oceanic relief (bathymetric profile) with**
 250 **exponential fitting curve (red line) and respective differential equations, behavior of**
 251 **sedimentation – deposition processes and physical-reworking patterns in the coastal**
 252 **zone and ACS; B) Distribution pattern of the SiO₂/Al₂O₃ ratio in the coastal zone and**
 253 **continental shelf with respective parabolic fitting curve (red line of tendency) and**
 254 **equation.**

255

256 **Table 1. Some characteristics of the sediment and pore water determined at the ACS**
 257 **(minimum and maximum values by zone).**

	Sediment					Pore water				
	Water depth	Porosity	Sand	Silt+Clay	OC	Salinity	pH	O ₂	Fe ²⁺	Fe ³⁺
	m	ml/cm ³	%	%	%	u.s.		%	mmol/L	mmol/L
ACS*	40.0	0.25	18.6	5.8	0.32	35.5	7.99	22.79	0.02	0.04
	98.5	0.40	94.2	81.4	1.78	38.4	8.21	57.60	0.03	0.05

CZ	4.5	0.66	9.4	80.6	0.46	4.9	6.51	5.64	0.04	0.04
	8.3	0.70	19.4	90.6	2.70	6.0	7.84	18.63	0.06	0.07
Inner	40.0	0.25	18.6	70.7	0.55	35.5	7.99	22.79	0.03	0.04
	42.2	0.40	29.3	81.4	0.88	37.7	8.21	38.54	0.03	0.05
Outer	72.4	0.28	43.9	5.8	0.32	36.3	8.03	39.37	0.02	0.04
	98.5	0.34	94.2	56.1	1.78	38.4	8.18	57.60	0.02	0.05

258 *ACS= sites 1 to 3 plus 5; CZ= sites 4 plus from 6 to 10; Inner= 3 and 5; Outer= 1 and 2.

259 4.2. Distribution of trace elements

260 The trace metal contents varied between Cr 36.5 – 86.4 (71.0±13.2); Pb 54.2 – 108.0
 261 (85.9±17.3); Ni 15.8 – 34.0 (25.1±6.1); and Zn 76.0 – 135.0 (108.0±21.7) mg/kg and Hg 66.0
 262 – 113.2 (77.8±11.4) ng/g (Figure 3A). The following behaviors were observed: 1) tendency
 263 to greater fraction of fine sediments in the inner shelf by direct influence of the high
 264 sedimentary load of the Amazon River mouth; 2) absence of OM in the sediments of the
 265 outer shelf by the continuous flow of the ocean currents from southeast to northwest; 3) a
 266 strong seasonality in the volume of sediment transported due to rainfall. The concentration
 267 of trace metals in the sediments followed the same convergence observed for the sediment
 268 flow, establishing a pattern with higher levels of trace metals in the CZ and inner shelf, and
 269 lower levels in the outer shelf (Figure 3B).

270 An important aspect in the flow of metals is the high capacity of metallic adsorption by the
 271 clay minerals in the sedimentary transport regime (discussed in the item 4.1). The high
 272 cation exchange capacity observed in the clay and OM particles, associated to the slightly
 273 acidic pH conditions in the fluvial-marine system, contributed to the storage of the trace
 274 metals especially in the inner shelf, as bivalent forms. This explains the positive correlation
 275 pattern calculated for OM, clay and trace elements. The Pearson correlation indexes
 276 calculated between OM and trace elements ranged from 0.516 Hg to 0.783 Ni (Table 2).
 277 There was also observed a significant correlation between OM and fine clay particles
 278 (0.776). In relation to the adsorption and desorption processes of the particles, the increase
 279 of the silicate load in the sediments of the outer shelf reduced the OM and clay contents
 280 and, consequently, of trace elements available for mobilization. The bioavailability of a trace
 281 metal, and consequently its toxicity, both depend on the form in which the metal is found
 282 (degree of speciation). Factors such as pH, Eh, alkalinity, degree of oxidation, suspended
 283 solids (OM and clay minerals), oxygen and temperature interfere with the
 284 mobility/precipitation ratio of trace metals. The pH has an important controlling role in the
 285 precipitation of the metallic elements through its ability to attack the minerals of rocks, soils
 286 and sediments [22], inducing the leaching or solubilization of the metals. During the leaching
 287 process, oxygen can be partially consumed to oxidize OM and reducing it to simpler
 288 inorganic fractions. Thus, the contribution of O₂ transferred from the cooler ocean currents to
 289 the sedimentary layer, especially in the first half meter, interferes in the OM-metals and clay-
 290 metals adsorption mechanism, a tendency observed in the negative correlation between the
 291 parameters. The depth of the sedimentary bed also showed a significant correlation, in this
 292 case with OM, sedimentary fractions, pH and salinity (Table 2).

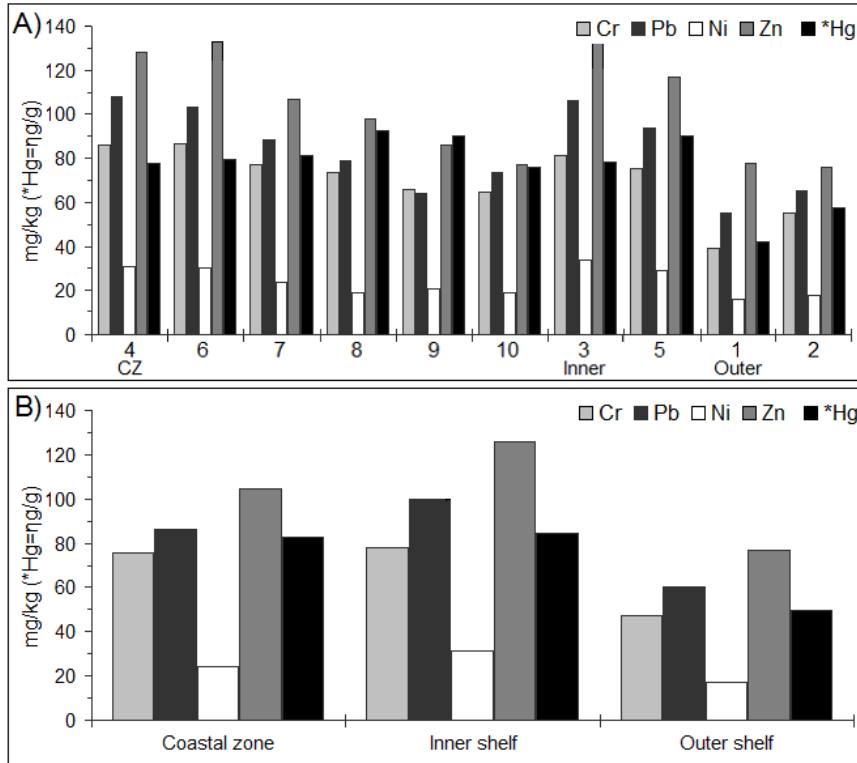
293 A normalization index was applied to the absolute values in order to establish the
 294 importance or 'weight factor' (F_w) of each parameter under the distribution and mobility of
 295 trace elements in the studied area. The normalization to establish a 'weight factor' is a
 296 practice usual in the creation of indexes such as the Water Quality Index, first applied by [27]
 297 for the National Sanitation Foundation (US NSF). Equation 8 presents the applied
 298 normalization calculation. The numerical values in front of each parameter indicate their
 299 'weight' of importance in the general tendency, and the signal (positive or negative) of each
 300 parameter indicates if the proportionality was direct or indirect in relation to the concentration

301 of trace elements in the sediments. The results suggest that the mobility of Cr, Ni and Zn is
 302 strongly related to the depth and location of sampling sites; sand, clay, OM and OC levels,
 303 and the DO concentration (Table 3).

304
$$F_w = \frac{Avr \times (SD)^2}{Max^2 - Min^2} \quad (eq.8)$$

305 Were: F_w = weight factor; Avr= average; SD= standard deviation; Max= maximum and Min=minimum.

306



307

308 **Fig. 3. Medium concentration and trend of the trace metals in the CZ and ACS, Blue**
 309 **Amazon – Brazil.**

310 **4.3. Diagenetic processes**

311 The series of physical-chemical transformations of OM, occurring in the water and sediment
 312 compartments, including pore water, is known as diagenesis. It is an essential process for
 313 the cycling of nutrients, allowing the renewal of marine life. In the diagenesis, several redox
 314 reactions occur due to the decomposition of OM by bacterial activity (reactions of Froelich et
 315 al. [28], whose main regulating factor is the concentration of DO in the sedimentary layer,
 316 especially in pore water. In aquatic sediments it is usual to continuously produce organic
 317 compounds through decomposition, by aerobic and anaerobic pathways, as well as
 318 mineralization of OM from the breathing and fermentation processes. Add to this
 319 autochthonous organic load the volume of organic compounds carried by the streams,

320 especially bottom streams, and deposited over an area, incorporating organics compounds
 321 into the processes mentioned above.

322 **Table 2. Pearson's Correlations:** bold correlations are significant at $p < 0.050$ and $n = 110$
 323 (values with 3 decimals $\pm .xyz$).

	Depth	OM	OC	IC	Sand	Silt	Clay	Si/Al	DO	O ₂ %	pH	Sal	Cr	Pb	Ni	Zn
Depth	1.0															
OM	-0.703	1.0														
OC	-0.476	0.875	1.0													
IC	.424	-0.718	-0.860	1.0												
Sand	0.915	-0.715	-0.556	.343	1.0											
Silt	-0.737	.383	.205	-0.202	-0.912	1.0										
Clay	-0.944	0.776	.537	-0.386	-0.958	0.760	1.0									
Si/Al ¹	0.803	-0.780	-0.692	.085	0.937	-0.863	-0.892	1.0								
DO	-0.464	-0.719	-0.677	-0.704	-0.145	.082	.233	.105	1.0							
O ₂ %	-0.299	-0.644	-0.525	-0.312	.011	-0.125	.081	.249	0.948	1.0						
pH	0.686	-0.713	-0.754	0.711	.565	-0.429	-0.599	.293	-0.531	-0.419	1.0					
Sal ²	0.882	-0.830	-0.583	.522	0.849	-0.466	-0.709	.444	-0.801	-0.662	0.755	1.0				
Cr	-0.565	0.632	0.601	-0.226	-0.715	0.738	0.729	-0.840	-0.408	-0.307	.070	-0.476	1.0			
Pb	-0.258	0.617	.540	-0.507	-0.425	.490	.437	-0.650	-0.592	-0.444	.418	-0.229	0.909	1.0		
Ni	-0.034	0.783	0.666	-0.612	-0.674	.529	.340	-0.522	-0.758	-0.473	.573	-0.474	0.794	0.926	1.0	
Zn	-0.041	0.732	0.663	-0.611	-0.231	0.634	.337	-0.470	-0.650	-0.564	.586	-0.409	0.821	0.945	0.961	1.0
Hg	-0.515	.516	.497	.013	-0.691	0.809	0.624	-0.714	-0.324	-0.251	.070	-0.489	0.789	0.705	0.627	.573

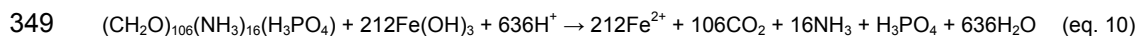
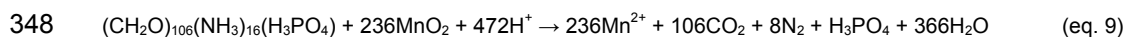
324 ¹ SiO₂/Al₂O₃; ² Salinity.

325 **Table 3. Weight factor (F_w) of the parameters analyzed in the distribution and mobility**
 326 **of trace elements.**

depth	OM	OC	IC	sand	silt	clay	Si/Al	DO	O ₂ %	pH	sal	Cr	Pb	Ni	Zn	Hg	
	-0.9	0.9	0.8	-0.6	-1.0	0.6	0.8	-1.0	-0.8	-0.6	0.1	-0.3	0.8	0.6	0.8	0.7	0.6

327 *Bold= values with significance at $p < 0.050$.

328 The relationship between the production and consumption of organic material defines the
 329 metabolism of an ecosystem, in this case benthic or sedimentary. In the euphotic zone, the
 330 processes of production exceed the mineralization in the diurnal phase [$\Delta(\text{CO}_{2T})_b = -n$],
 331 reversing the direction of the reaction at night [$\Delta(\text{CO}_{2T})_b = +n$]. In addition to O₂, physical and
 332 physical-chemical factors such as stream flow, sediment porosity, sedimentation rate, water-
 333 sediment interface temperature, pH, alkalinity, cation exchange capacity (CEC), trace
 334 element concentration, OM, respiration rate and intensity of benthic biological activity
 335 determine the way diagenesis occurs, especially in the time of nutrient regeneration rate. By
 336 analyzing the sampling sites by zoning, it was possible to identify areas of low O₂ content,
 337 with an increase in CO_{2T} levels. These results suggest moments of reduction of Fe³⁺ and
 338 Mn⁴⁺ (equations 9 and 10) [28], especially in areas with high OM content and protected from
 339 currents such as site 4 below 0.2 meters (Figure 1). Degradation of the organic matter by the
 340 reduction of Mn⁴⁺ (eq.9) is thermodynamically more favorable than the reduction of Fe³⁺
 341 (eq.10). However, the iron reduction pathway is considered to be more important for the
 342 mobility and/or co-precipitation of trace elements in the coastal zone and inner shelf,
 343 because the total Fe concentration in the Amazonian continental waters is about 100 times
 344 higher than the concentration of manganese. The mean total Fe and Mn concentration
 345 determined in the Amazon River waters is 1.3 – 3.4 mgFe/L and 0.009 – 0.08 mgMn/L
 346 (Darwich and Aprile, unpublished data). Sequence of oxidant species observed in the
 347 sedimentary layer [28]:

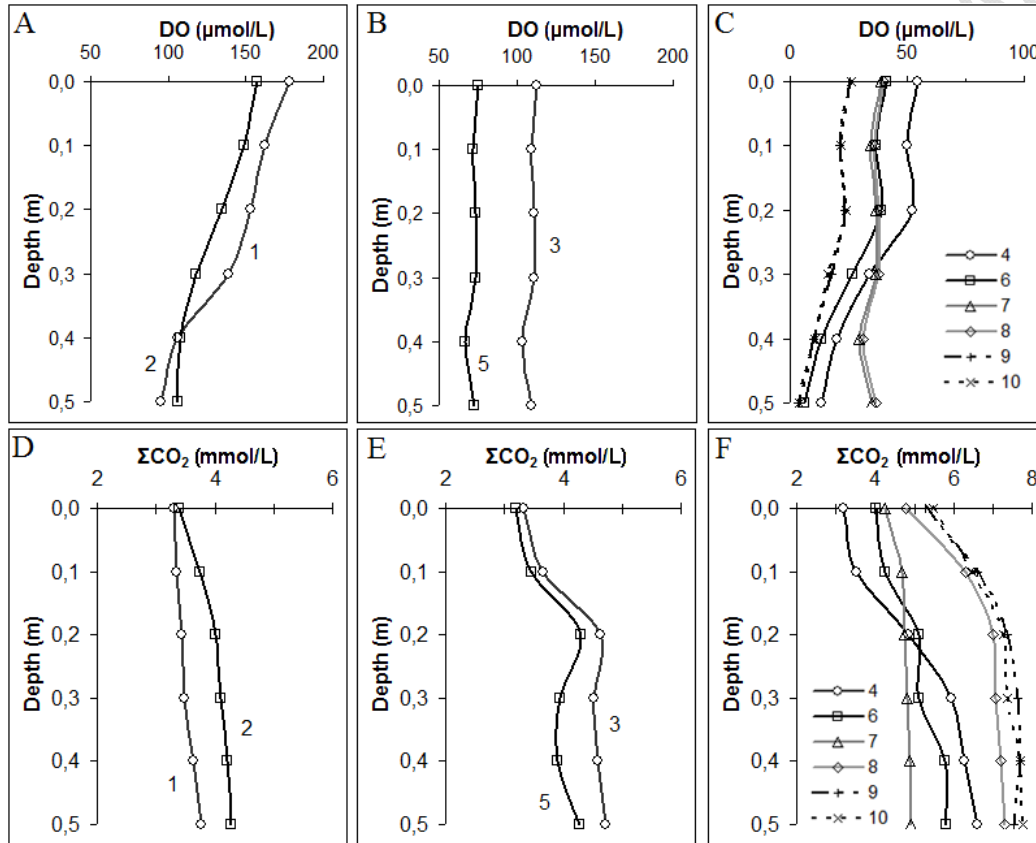


350 Although in the coastal zone and inner shelf areas occurs large deposition of OM, factors
351 such as slightly alkaline pH and low interstitial O₂ levels may be contributing to the reduction
352 of mobility of trace elements. Considering that part of the DO content is being consumed by
353 the OM oxidation, the process of deposition and reduction of the metallic mobility intensifies,
354 ensuring that this sedimentary layer acts preferentially as a storage compartment (stock) of
355 trace elements. Vertical profiles of the O₂ and ΣCO₂ contents in the pore water of the
356 sedimentary layer of the sampled sites were elaborated (Figure 4). In general, the sandy
357 sedimentary layer had a greater flow of oxygenation than the mud layers of the coastal zone
358 and inner shelf. DO contents in the 0.0 – 0.5 m ranged from 95.6 – 178.1 μmol/L on the
359 outer shelf; of 66.5 – 112.5 μmol/L on the inner shelf; and 3.1 – 54.4 μmol/L in the coastal
360 zone (Figure 4). The bottom currents in the outer shelf, cooler and oxygenated, they
361 interfered in the sedimentary O₂ flux, facilitated by the porosity of the sandy sediments. It
362 can be pointed out that the diffuse oxygen flux in the sediments was directed by the
363 consumption in the oxidation process. The oxidation of organic matter in fluvial-marines
364 sediments is considered the most important form of respiration in fluvial-marine sediments
365 [29]. Besides, another factor may be contributing to diffuse oxygen flow, in this case a
366 biological action involving benthic respiration, especially in coastal sediments. Studies on
367 oxygen flow and oxireduction of nitrogenous and sulfated forms (NO₃ and SO₄) performed in
368 the same region demonstrated the importance of the benthic respiration in diagenetic
369 processes [29-31]. In general, aerobic respiration takes place in the oxic surface layer and is
370 followed by nitrate and sulfate reductions. However, in coastal sediments the oxic zone often
371 is only a few millimeters thick, as suggest the studies of [12] and [28], and exactly as
372 observed in the sediments of the coastal zone and inner shelf of the ACS, where the
373 anaerobic respiration becomes dominant. Besides, much of the oxygen uptake is used to
374 reoxidate the products of anaerobic respiration as H₂S, NH₄⁺ and CH₄ at the oxic/anoxic
375 interface of the sediment [32].

376 The mineralization of the anaerobic organic matter involves several oxidation processes,
377 consuming nitrates, Fe and Mn oxides, sulfates and carbonic acid to form CO₂ and
378 fermentation, in this case with formation of CH₄ (methanogenesis). Due to its greater stability
379 in relation to H₂S and SO₄²⁻, the CO₂ becomes an important indicator of diagenetic
380 processes. In general, is considerate for analysis the sum of all dissolved carbonate forms,
381 which are defined as total inorganic carbon or CO_{2T}. The concentration oscillation of both
382 free CO₂ and CO_{2T} depends directly on the production and consumption in the processes
383 already mentioned, pH, alkalinity of the carbonates and ionic composition of the water. The
384 carbonate content, which interferes with pH and alkalinity, has as main source in the marine
385 environments the contribution carried by the waterways and biogenic production, whose
386 main raw materials are plankton and mollusks. In relation to carbonate content, in the
387 Amazonian plain the main source of carbonate is predominantly HCO₃⁻ [33]. The biogenic
388 production of carbonate in shallow waters and its dissolution in deep waters causes a
389 dynamic equilibrium system, affected by ocean currents, and that controls, among other
390 factors, the concentration of total inorganic carbon in the system. The CO_{2T} contents
391 presented some variability as a function of zonation, ranging from 3.3 – 4.3 mmol/L in the
392 outer shelf; of 3.3 – 4.7 mmol/L on the inner shelf; and 3.2 – 7.8 mmol/L in coastal zone
393 sediments (Figure 4). The higher CO₂ levels in the sediments are associated with
394 decomposition processes and complete oxidation of organic matter and mineralization
395 partially anaerobic of the sedimentary particles. All the sampling sites showed a
396 considerable capacity for a rapid change in pore water constituents associated with the
397 remineralization processes, suggesting the presence of abundant organic compounds,
398 especially in the inner shelf that, as mentioned above, act primarily as a storage

399 compartment of thin sediments, depending on their morphology and flow direction. At some
 400 sampling sites, the exponential decay of O₂ occurred simultaneously to CO₂ production,
 401 especially at depths of 0.0 – 0.2 meters in the sedimentary layer. This behavior reflects the
 402 nature of particle deposition and reworking of particles. It should be remembered that the
 403 samplings and measurements were carried out during the months of the lowest flow in the
 404 Amazon and Pará rivers and at the ACS. Thus, it is plausible to believe that seasonality can
 405 alter the flow pattern of oxygen as well as CO₂ during the hydrological year, especially
 406 during the periods of higher flow of the Amazon River, when the sediment load transported
 407 can reach double volume, as has been suggested by [10] and [13].

408



409

410 **Fig. 4. Vertical profile of DO (μmol/L) and ΣCO₂ (mmol/L) according to the zoning**
 411 **process: A) and D) outer shelf; B) and E) inner shelf; C) and F) coastal zone.**

412

413 4.4. Sedimentary incubation

414 Incubation tests can be classified into open and closed systems. In the open system the loss
 415 of CO₂ by diffusion is allowed, which does not return to the system. However, the closed
 416 system is often questioned by 'imprisoning' the gases, preventing the changes at the water-
 417 sediment interface. The fact is that both tests have positive and negative points, and it must
 418 be assumed that there is an imprecision in the results. The great trump of incubation tests,

419 however, is the ability to quantitatively estimate the processes involved. It is based on this
420 perspective that a closed test was applied to estimate the net productivity and mineralization
421 content of OM in the coastal zone and ACS.

422 The variation of the $\text{CO}_{2\text{T}}$ and O_2 in the waters ($\Delta\text{CO}_{2\text{T}}(t)$ and $\Delta\text{O}_2(t)$), including the pore
423 waters, is controlled not only by the biological processes but also by the diffusion rate of the
424 gases in the interface zone ($\Delta(\text{CO}_{2\text{T}})_a$ and $\Delta(\text{O}_2)_a$), and the facilitation or not of the gas flow
425 as a function of the degree of sedimentary porosity. Thus, the study of the diagenetic
426 processes involving the production and mineralization from the CO_2 and O_2 variations in the
427 water should be understood as an estimate, since there are several factors controlling the
428 concentration and flow of these gases in the sediments, including hydrodynamics and
429 seasonality. The closed incubation technique attempts to minimize the problem of gas
430 exchange. Despite this, incubation reduces the flow of biogenic elements. The system's
431 buffering capacity is of great relevance to the results, since any change in pH and alkalinity,
432 especially alkalinity of carbonate (Alc_c), interferes with the concentrations of H_2CO_3 , HCO_3^-
433 and CO_3^{2-} , and consequently with $\text{CO}_{2\text{T}}$ levels. It is tried to minimize this variation,
434 considering that the chemical reactions and the diffusions present kinetics of the same
435 order. Thus, when CO_2 adsorption occurs, a part of the CO_2 that enters the system is
436 transformed into carbonates, and when the CO_2 desorption occurs, a fraction of carbonates
437 from the system is converted into CO_2 . Incubation tests confirmed that the range of 0.0 – 0.2
438 m is essentially the most active from the point of view of sediment reworking by the flow and
439 inflow of the dissolved gases. As expected, $\text{CO}_{2\text{T}}$ rates increased rapidly during the
440 incubation period. Increasing the concentration of inorganic carbon forms may mean an
441 increase in aerobic decomposition rates (complete decomposition), due to the increase in
442 the supply of reactive organic compounds. Generally, the saturation of mineral carbonates
443 and other forms of inorganic carbon are quite high in the sediments from ACS, as were
444 observed by [2,12].

445 In the comparison of the results between the incubation of sediments from site 1, sandy and
446 under strong influence by marine currents, to site 4, mud and located in protected area with
447 marked sedimentation, the amplitude of variation for the incubation period ($t_0 \rightarrow t_{96}$) was
448 much higher at site 4. The $\Delta\text{CO}_{2\text{T}}$ determined were respectively; site 1= 1.44 mmol/L and
449 site 4= 4.94 mmol/L (Table 4), suggesting that the net mineralization exceeded the net
450 production of organic matter to [$\Delta(\text{CO}_{2\text{T}})_b > 0$ for $\Delta(\text{O}_2)_b < 0$]. The coefficient of activity (I)
451 also showed a greater amplitude of variation in site 4 ($\Delta I = 3.26$ meq/L) compared to site 1
452 ($\Delta I = 1.81$ meq/L). The activity coefficient is a function not only of the chemical species
453 present, but also of the ionic interactions in pore water. In silica sediments, the ionic
454 interactions are weak and easily disrupted by the current underflow, which eventually
455 penetrates the sediments due to their high porosity. Already in silt-clayey and clay-silty
456 sediments, the low porosity (<0.7 ml/cm³) reduces the mobility of the mineral elements,
457 accentuating the ionic interactions, which present strong connections, especially cationic,
458 with the negative external surface of the particles of clay and organic matter. The ionic
459 forces (F_i), determined as a function of their logarithms, followed the same trends, being
460 greater in the mud sediments. These behaviors are confirmed in the CEC analysis. Another
461 important aspect is the variation rate in the productivity of NH_4^+ ions (Table 4), which showed
462 influx in sandy sediments (site 1 = -9 $\mu\text{mol/L}$), and high efflux for mud sediments (site 4 = 53
463 $\mu\text{mol/L}$).

464 Extrapolating the results of the incubation test to the study area, it is possible to establish
465 some hypotheses: 1) the flow of marine currents at site 1 may be allowing the aerobic
466 oxidation in these sedimentary layers, with the nitrification route more pronounced than the
467 ammonification rate; 2) in the region of the coastal zone and inner shelf the routes of
468 oxidation and reduction may be alternating according to the physical, physical-chemical and

469 seasonal factors; 3) in the coastal zone and inner shelf the net mineralization rate has
 470 exceeded the net production rate of organic matter, since the calculations show $\Delta(\text{CO}_{2\text{T}}) > 0$
 471 for $\Delta(\text{O}_2) < 0$ (Table 4) for the vector from site 1 to site 4 (Figure 1). It should be considered,
 472 however, that the rate of sedimentation or continuous contribution of sediments from the
 473 Amazon River to the inner shelf is immense, as already discussed.

474 Daily fluctuations in the rate of NH_4^+ production at the same site, with changes in the axis of
 475 orientation of influx - efflux (nitrification/ammonification) are not uncommon, having been
 476 observed even in incubation tests [29,30]. In the specific case of the sediments located in
 477 the axis of orientation of the vector shown in figure 1, it is believed that the great difference
 478 in porosity and OM contents of the sediments, associated to the depth of the layer, were the
 479 predominant factors in the change of the orientation axis of inflow-efflux. This was confirmed
 480 by determination of iron fractions. Most of the time $\text{Fe}^{2+}/\text{Fe}^{3+}$ ratio was < 1.0 throughout the
 481 sedimentary profile (Figure 5), suggesting a mild to moderate oxidation pattern in the first 0.4
 482 m, especially for outer shelf sites (sampling sites 1 and 2). A sensitive reduction in the
 483 degree of oxidation of the ferric ions was observed in sites 2 and 3 from 0.4 m. However,
 484 site 4 (Silt + Clay $> 80\%$) presented higher iron ratio, with $\text{Fe}^{2+}/\text{Fe}^{3+} > 1.0$, indicating a
 485 predominance of the maintenance of the reduced form of iron (Fe^{2+}), which by electric
 486 affinity remains in the sedimentary layer adsorbed the particles of clay minerals and organic
 487 compounds not totally mineralized. Metal profiles sensitive to oxidation variation, such as Fe
 488 and Mn, may indicate redox potential changes within the sedimentary layers, being
 489 influenced by the concentration of DO in the pore water. The pore water column can define
 490 alternate zones of oxidation and reduction of chemical species as a function of depth,
 491 according to sedimentation rates, oxygen demand, nutrients and microbiological processes
 492 [34]. The processes of dissolution and precipitation of minerals can affect the nutrient
 493 concentration (C, N and P) and trace elements in the sediments [8], because these chemical
 494 species may be being adsorbed by the surface of minerals as iron oxides and hydroxides.
 495 The behavior of the trace elements in the bottom sediments is strongly associated with
 496 organic matter rates; pH (increase of the pH implies increase of the metallic adsorption); O_2
 497 content; redox potential; seasonality (flow of alternating currents); and diagenetic processes,
 498 which occur in the fluvial-marine system. In this case, three routes of adsorption of trace
 499 elements to the iron in the sediments and pore water can be established, taking into account
 500 the depth and oxygen content: 1) adsorption in Fe^{3+} oxides and hydroxides, especially at the
 501 water-sediment interface and with increased metal mobility; 2) dissolution of Fe^{2+} oxides and
 502 hydroxides in the layers of less interference of O_2 , in this case the trace elements may follow
 503 the oxidative route towards the interface, or to stay associated with reduced forms (S^{2-}) and
 504 follow the co-precipitation way; and 3) fixation on the mineral surface or precipitation in the
 505 autigenic mineral phase, in or near the anoxic environment (Figure 5). Reactive trace
 506 elements such as Cu, Ni and Zn may have their concentrations controlled by co-precipitation
 507 with Fe sulfides, which would result in the reduction of the metallic mobility of these
 508 elements. Comparing the trace element contents with the vertical distribution profile of the
 509 iron fractions, it was possible to evidence an increase in trace element concentrations in Fe
 510 reduction zones, indicating processes of desorption of iron oxides and hydroxides, and
 511 mineralization of organic matter.

512 **Table 4. Estimates of net production and net mineralization of organic matter from the**
 513 **incubation test (t= 96h) for sites 1 (outer shelf) and 4 (coastal zone).**

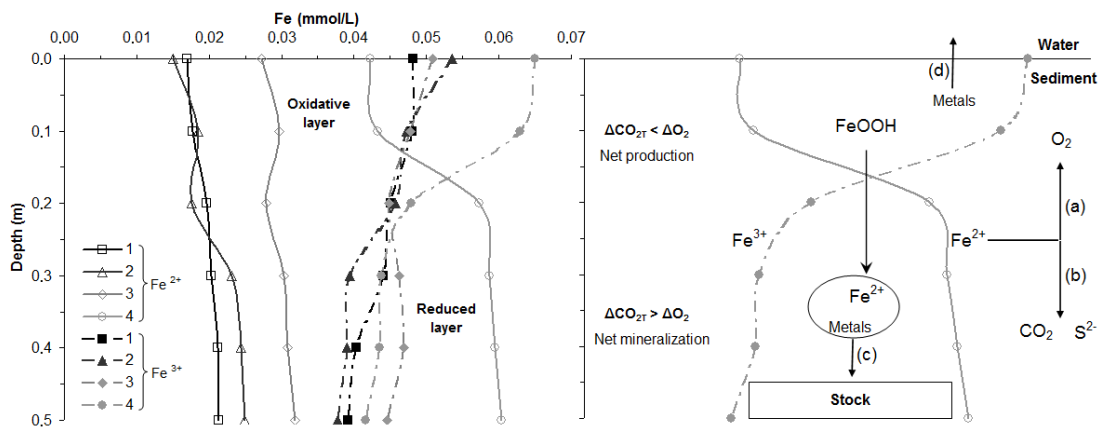
Site	Depth (m)	$[\text{CO}_{2\text{T}}]$ (mmol/L)		$\Delta\text{CO}_{2\text{T}}$ (mmol/L)	ΔI^* (meq/L)	F_i^{**} (log)	ΔNH_4^+ ($\mu\text{mol/L}$)	$\text{Fe}^{2+}/\text{Fe}^{3+}$
		t_0	t_{96}					
1	0.0	3.30	4.10	1.44	1.81	-1.50	-9	0.35

1	0.5	3.50	4.80					0.54
4	0.0	3.60	6.60	4.94	3.26	-0.48	53	0.65
4	0.5	3.80	8.70					1.45

514 *Activity coefficient variation for t=96h

515 **Ionic force defined by [19]

516



517

518 **Fig. 5. Vertical profile of the Fe^{2+} and Fe^{3+} fractions in the pore water from sediments**
519 **located in the vector 1 – 4 of the ACS, and indication of the possible transport routes**
520 **of the associated trace elements.** Legend: a) decomplexing; b) co-precipitation; c) fixation;
521 d) mobilization.

522 5. CONCLUSION

523 Establishing that the study area is comprised between the coastal zone, which receives
524 directly the sedimentary contribution from the discharges of the Amazonas and Pará rivers,
525 and the outer shelf, which is under direct influence of the ocean currents (see Figure 1), was
526 able to the following conclusions: 1) There is a strong zonation in the sedimentary transport
527 and deposition processes, influenced by the granulometry and texture of the sediments, and
528 the fluvial-marine currents, which alternate in direction seasonality. Thus, it was possible to
529 identify that the sediments of the coastal zone and inner shelf are predominantly silt-clayey
530 and clay-silty as opposed to sandy and sand-silt sediments of the outer shelf. 2) The trace
531 elements presented a distribution and concentration pattern equivalent to that of the
532 sedimentary distribution pattern, with higher metallic contents in the deposits of clay and
533 organic matter of the coastal zone and inner shelf. 3) The determination of a weight factor
534 (F_w) calculated to estimate the degree of importance of each physical and physical-chemical
535 parameter in the distribution and mobility of trace elements showed that these elements
536 were strongly related to the depth and location of sampling sites, sand, clay, OM and OC
537 levels, and DO concentration, especially to Cr, Ni and Zn metals. 4) The vertical distribution
538 of O_2 and CO_2 and the Fe^{2+}/Fe^{3+} ratio in the pore water suggest a predominance of organic
539 matter oxidation in the sedimentary layer between 0.0 and 0.2 m, with partially anaerobic
540 mineralization of the mud sediments below 0.4 m, especially in the coastal zone and inner
541 shelf. However, the results indicate that there may be very significant differences between
542 aerobic and anaerobic degradation of organic matter. 5) Increases in trace element
543 concentrations were observed in Fe reduction zones, indicating processes of desorption of
544 Fe oxides and hydroxides and net mineralization of OM. 6) The results of the incubation test
545 indicated that $\Delta(CO_{2T}) > 0$ for $\Delta(O_2) < 0$, suggesting that especially for the coastal zone and

546 inner shelf the net mineralization rate has exceeded the net production rate of organic
547 matter.

548 **COMPETING INTERESTS**

549 Authors have declared that no competing interests exist.

550 **AUTHORS' CONTRIBUTIONS**

551 All authors participated of the samples collection, date and statistical analysis and wrote the
552 first draft of the manuscript.

553 **CONSENT**

554 All the authors accepted the terms for publication, and we agree that, if the manuscript is
555 accepted for publication, we'll transfer the copyright-holder of the manuscript to BJECC and
556 SDI, including the right of total or partial reproduction in all forms and media. We informed
557 also that if accepted, the manuscript will not be published elsewhere including electronically
558 in the same form, in English or in any other language, without the written consent of the
559 copyright holder.

560 **ETHICAL APPROVAL**

561 This section is not applicable in this manuscript.

562 **REFERENCES**

- 563 1. Shokes RF. Rate-dependent distributions of lead-210 and interstitial sulfate in
564 sediments, of the Mississippi River Delta. Department of Oceanography, Texas A&M
565 University, Report 76-1-T, College Station; 1976, 96 pp.
- 566 2. Aller RC, Mackin JE, Ullman WJ, Hou WC, Min TS, Cai JJ, Nian SU, Zhen HJ. Early
567 chemical diagenesis, sediment-water solute exchange, and storage of reactive organic
568 matter near the mouth of the Changjiang, East China Sea. *Continental Shelf Research*
569 1985; 4:227-251.
- 570 3. Shaw TJ, Gieskes JM, Jahnke RA. Early diagenesis in differing depositional-
571 environments – the response of transition-metals in pore water. *Geochimica et*
572 *Cosmochimica Acta* 1990; 54(5):233-1246.
- 573 4. Carman R, Rahm L. Early diagenesis and chemical characteristics of interstitial water
574 and sediments in the deep deposition bottoms of the Baltic proper. *Journal of Sea*
575 *Research* 1997; 37:25-47.
- 576 5. Ziebis W, Forster S. Impact of biogenic sediment topography on oxygen fluxes in
577 permeable seabeds. *Mar. Ecol. Prog. Ser.* 1996; 140:227-237.
- 578 6. Schulz HD. Quantification of early diagenesis: dissolved constituents in marine pore
579 water. In: Schulz HD, Zabel M. (Eds.). *Marine Geochemistry*. New York: Springer-
580 Verlag; 2006, pp. 85-99.
- 581 7. Breitzke M. Physical Properties of Marine Sediments. In: Schulz HD, Zabel M. (Eds.).
582 *Marine Geochemistry*. New York: Springer-Verlag; 2006, pp. 29-33.
- 583 8. Siqueira G, Aprile F, Irion G, Marshall B, Braga E. Source and distribution of mercury in
584 sediments of the Brazilian Amazon Continental Shelf with influence from fluvial
585 discharges. *American Chemical Science Journal* 2016; 15:1-15.
- 586 9. Siqueira GW, Aprile FM. Distribution of total mercury in sediments from Amazon
587 Continental Shelf – Brazil. *Acta Amazônica* 2012; 42:259-268. Portuguese

- 588 10. Meade RH, Dunne JE, Richey U, Salate E. Storage and remobilization of suspended
589 sediment in the lower Amazon river estuary. *Nature* 1985; 278:161-163.
- 590 11. Kuehl SA, DeMaster DJ, Nittroucr CA. Nature of sediment accumulation on the Amazon
591 continental shelf. *Continental Shelf Research*. 1986; 6:209-225.
- 592 12. Aller RC, Blair NE, Xia Q, Rude PD. Remineralization rates, recycling, and storage of
593 carbon in Amazon shelf sediments. *Continental Shelf Research* 1996; 16(516):753-786.
- 594 13. Gibbs RJ. The bottom sediments of the Amazon Shelf and tropical Atlantic Ocean.
595 *Marine Geology* 1973; 14:M39-M45.
- 596 14. Donagema GK, Campos DVB, Calderano SB, Teixeira WG, Viana JHM. (Orgs.).
597 *Manual of soil analyses methods*. Rio de Janeiro: Embrapa Solos 2011. Portuguese.
- 598 15. Jackson ML. *Soil chemical analysis*. Englewood Cliffs: Prentice-Hall; 1962, 498 pp.
- 599 16. Silva FC. *Manual of chemical analyses of soils, plants and fertilizers*. Embrapa Solos,
600 Embrapa Informática Agropecuária. Brasília: Embrapa Comunicação para
601 Transferência de Tecnologia; 1999, 370 pp.
- 602 17. American Public Health Association (APHA), American Water Works Association
603 (AWWA), Water Environment Federation (WEF). *Standard methods for the examination*
604 *of water & wastewater*. USA: APHA/AWWA/WEF; 2012, 22nd ed.
- 605 18. Mackin JE, Swider KT. Organic matter decomposition pathway and oxygen
606 consumption in coastal marine sediments. *J. Mar. Res.* 1989; 47:681-716.
- 607 19. Kielland J. Individual activity coefficients of ions in aqueous solutions. *Am. Chem. Soc.*
608 *Jour.* 1937; 59:1675-1678.
- 609 20. Garrels RM, Thompson ME. A chemical model for sea water at 25°C and one
610 atmosphere total pressure. *Amer. J. Sci.* 1962; 260:57-66.
- 611 21. Nittrouer CA, Sharara MT, DeMaster DJ. Variations of sediment texture on the Amazon
612 continental shelf. *Journal of Sedimentary Petrology* 1983; 53:179-191.
- 613 22. Salomons W. Long-term strategies for handling contaminated sites end large-scale
614 areas. In: Salomons W, Stigliani WM. (Ed.). *Biogeodynamics of pollutants in soil and*
615 *sediments: risk assessments of delayed and non-linear responses*. Environmental
616 *Science and Engineering Series*, Berlin: Springer; 1995, 352 pp.
- 617 23. Förstner U. *Sediment dynamics and pollutant mobility in rivers: An interdisciplinary*
618 *approach*. *Lakes & Reservoirs: Research and Management* 2004; 9:25-40.
- 619 24. Salomons W, de Rooij NM, Kerdijk H, Bril J. Sediments as a source for contaminants.
620 *Hydrobiologia* 1987; 149:13-30.
- 621 25. Förstner U. Non-linear release of metals from aquatic sediments. In: Salomons W,
622 Stigliani WM. (Eds). *Biogeodynamics of pollutants in soils and sediments: risk*
623 *assessment of delayed and non-linear responses*, Heidelberg: Springer Verlag; 1995,
624 pp. 247-298.
- 625 26. Horowitz AJ. *A Primer on Sediment-Trace Element Chemistry*, 2nd ed., Chelsea, MI:
626 Lewis Publishers, Inc., 1991.
- 627 27. Brown RM, McClelland NI. *Up from chaos: the water quality index as an effective*
628 *instrument in water quality management*. Michigan: National Sanitation Foudantion
629 1974.
- 630 28. Froelich PN, Klinkhammer GP, Bender ML, Luedtke NA, Heath GR, Cullen D, Dauphin
631 P, Hammond D, Hartmann B, Maynard V. Early oxidation of organic matter in pelagic
632 sediments of the eastern equatorial Atlantic: Suboxic diagenesis. *Geochim.*
633 *Cosmochim. Acta* 1979; 43:1075-1090.
- 634 29. Sorensen J, Jorgensen BB, Revsbech NP. A comparison of oxygen, nitrate and sulfate
635 respiration in coastal marine sediments. *Microb. Ecol.* 1979; 5:105-115.
- 636 30. Jorgensen BB, Sorensen J. Seasonal cycles of O₂, NO₃⁻ and SO₄⁻ reduction in estuarine
637 sediments: the significance of an NO₃⁻ reduction maximum in spring. *Mar. Ecol. Prog.*
638 *Ser.* 1985; 24:65-74.

- 639 31. Jorgensen BB, Revsbech NP. Oxygen uptake, bacterial distribution, and carbon-
640 nitrogen-sulfur cycling in sediments from the Baltic Sea-North Sea transition. *Ophelia*
641 1989; 31:29-49.
- 642 32. Jorgensen BB. The microbial sulfur cycle. In: Krumbein WE. (Ed.). *Microbial*
643 *geochemistry*. Oxford: Blackwell; 1983, pp. 91-12.
- 644 33. Aprile F, Darwich AJ, Siqueira GW, Ribeiro AA, Santos VC. Hydrological
645 characterization of a whitewater lake at Amazon floodplain - Brazil. *International*
646 *Research Journal of Environment Sciences* 2013; 2:44-53.
- 647 34. Vale C, Sundby B. The interactions between living organisms and metals in intertidal
648 and subtidal sediments. In: Langston WY, Bebianno MY. (Eds.). *Metal metabolism in*
649 *aquatic environments*. London: Chapman & Hall; 1998, pp. 19-29.

UNDER PEER REVIEW